

A Beam-Split and Gain-Enhanced Patch Antenna Using Metamaterial Superstrate for Wireless Communications

Bashar S. Bashar¹, Taha Ahmed Oleiwi², Zeti Akma Rhazali³, Halina Misran⁴, Marwa M. Ismail⁵, Bashar Bahaa Qas Elias⁵

^{1,3} Electrical & Electronic Engineering Department College of Engineering Universiti Tenaga Nasional Kajang, Malaysia.

² Islamic University Centre for Scientific Research, The Islamic University, Najaf, Iraq.

⁴ Nanoarchitectonic Laboratory Department of Mechanical Engineering Universiti Tenaga Nasional Kajang, Malaysia.

⁵ Department of Information and Communication Engineering, College of Information Engineering, Al-Nahrain University, Jadriya, Baghdad, Iraq.

Abstract: This paper proposes multiband antenna-based Metamaterial (MTM) for beam splitting and gains improvement. Here, the focus is on developing the smart antenna using a Metamaterial Superstrate technique for modern wireless applications. The proposed antenna consists of two patches, the first one has a square shape placed on a Taconic FR-30 substrate, followed by the second patch constructed as a meander ring with two stubs for increasing the generated frequency bands. At the end of the design process, the proposed patch seems U-shaped to ensure the antenna beam is splitting at the desired frequency bands. In addition, the capacitive coupling is used for exciting the second patch, whereas the first patch is excited by conduction with a 50 Ω discrete port. Furthermore, a metasurface layer is designed and mounted on the second patch as a superstrate to increase the antenna gain toward the bore-sight direction. The results show a maximum gain of 8 dBi at 4.2 GHz with maximum dimensions of 108 \times 108 mm². Moreover, this antenna operates at additional frequency bands (2.6 GHz, 4.2 GHz, and 5.6 GHz), with a minimum reflection coefficient of -16.8 dB, -12.3 dB, and -30.6 dB, respectively. The proposed antenna is designed and analyzed using the CST MWS simulator.

Keywords: patch antenna, metamaterial, superstrate, gain, beam splitting

Krpična antena z razcepljenim snopom in povečanim dobitkom z uporabo metamaterialne podlage za brezžične komunikacije

Izvleček: Članek predlaga večpasovno anteno na osnovi metamateriala (MTM) za razdelitev snopa in izboljšanje dobička. Pri tem se osredotočamo na razvoj pametne antene s tehniko metamaterialnega superstrata za sodobne brezžične aplikacije. Predlagana antena je sestavljena iz dveh krpic, prva je kvadratne oblike in je nameščena na substrat Taconic FR-30, sledi ji druga krpica, zgrajena kot meandrski obroč z dvema krakoma za povečanje generiranih frekvenčnih pasov. Predlagana krpica je v obliki črke U, da se zagotovi, da se antenski žarek razdeli na želene frekvenčne pasove. Poleg tega se za vzbujanje druge krpice uporablja kapacitivni sklop, medtem ko se prva krpica vzbuja s prevodnostjo z diskretnim priključkom 50 Ω . Poleg tega je zasnovana in nameščena metapovršinska plast na drugo krpico kot superstrat za povečanje ojačitve antene. Rezultati kažejo največje ojačenje 8 dBi pri frekvenci 4,2 GHz z največjimi dimenzijami 108 \times 108 mm². Poleg tega antena deluje v dodatnih frekvenčnih pasovih (2,6 GHz, 4,2 GHz in 5,6 GHz) z najmanjšim koeficientom odboja -16,8 dB, -12,3 dB in -30,6 dB. Predlagana antena je zasnovana in analizirana s simulatorjem CST MWS.

Ključne besede: krpična antena, metamaterial, superstrat, ojačenje, delitev žarka

1 Introduction

The rapid development of wireless communications pushed the user to become greedy to obtain the highest capacity and high speed, and this rapid development in the next generations of communications [1]. The fifth generation (5G) helped change the concept of speed and high productivity. On the other hand, this development needs a high gain. Therefore, arrays are proposed in several research to get the best results in terms of high gain and the ability to change the system's characteristics and avoid interference [2, 3]. Multi-beam antennas are used in many fields, **whether in communications or in other areas**. These antennas are assembled in fifth-generation stations to obtain better compatibility, high capacity, and efficiency [4, 5]. In wireless communications, especially in the fifth generation, the antennas must be different from the rest of the generations in terms of weight and size. **Therefore, microstrip antennas are used** to improve the performance of the antennas with their integration using planar manufacturing [6, 7].

The proposed structure consists of three main parts, as shown in Fig. 1. The first part is the microstate antenna based on a square patch. The antenna is excited with a 50Ω input impedance along with weight. The second part is represented as a Hilbert U-shaped structure of the second iteration. The proposed Hilbert is designed as an open fractal which excited with T-ring stubs, as shown in figure 1 (c). The loop of two rings helps achieve minimum field fringing [8]; this would realize surface current mitigation to a certain direction that reduces the back radiation [9]. Besides that, the advantage of introducing the proposed T-ring steps is accumulating electrical charges which excites the proposed Hilbert U-shaped capacitively to improve the bandwidth [10].

Meanwhile, the proposed U-turns are proposed to achieve multiple frequency harmonic generation from the fractal corner. Moreover, fractal geometric provides a significant size reduction [11]. Finally, the proposed antenna has a symmetrical profile around the length and an asymmetrical shape along the weight. Hence, the basic antenna radiation would be asymmetrical around the importance of generating beam splitting [12]. This helps the designer develop a stigmatized wave configuration [13]; the antenna beam could be focused significantly with minimum size reduction, which will be further explained in the next paragraph after the Metasurface layer introduction and realize beam splitting at the same time. This is due to the creation of two areas with high concentrations of the surface current on the second patch, which inherently increases the beam splitting around the antenna length [14, 15].

Next, the metamaterial (MTM) is designed and integrated with a proposed antenna to maximize the antenna gain in the bore-sight direction [16]. Finally, the

proposed metamaterial is structured in an asymmetrical form.

This paper is organized as follows. Section II presents the antenna configuration and design procedures for the proposed structure, followed by simulation results in Section III. Then, the metamaterial cases results are demonstrated in section IV. Finally, some concluding remarks are discussed in Section V.

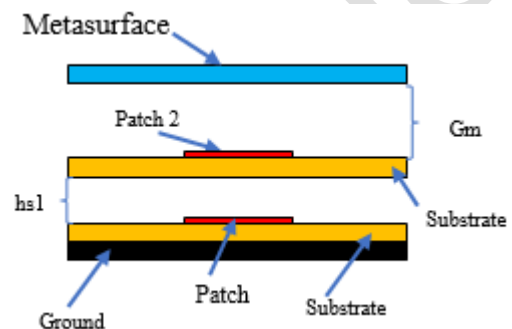


Figure 1: Schematic view of the antenna.

1.1 Design of U-shape cell

In this section, the second patch with a U-shape structure is designed, and its dimensions are (a width of 71.28 mm and a length of 66.47 mm). Different attempts are performed to adjust the dimensions of the U-shape patch length and width for various thicknesses to get better results of the antenna performance. The basic structure of the U-shape proposed antenna is portrayed in Fig.2.

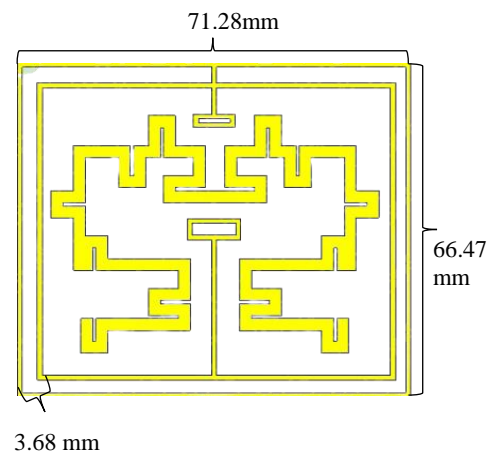


Figure 2: U-shape antenna.

1.2 Design of microstrip patch antenna

Several methods have been proposed in designing **patch antennas (PN)**, and the most popular model is

the **transmission line model (TL)**. It models the rectangular patch (RP) as two slots separated by a low impedance transmission line (Z_c) of length L . In this study, the proposed patch antenna is designed using a Taconic FR-30 substrate with a width and length of 50 mm, respectively (see Fig. 3).

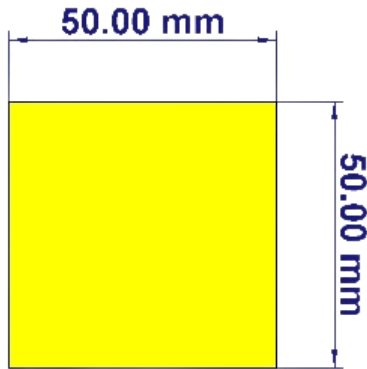


Figure 3: Patch dimensions.

1.3 Metamaterial unit cell structure

The MTM is used with a certain distance from the substrate[17], as shown in Fig. 1. This method prepares the radio transmitters in the same direction as the antenna and works to increase the antenna gain[18]. Designing MTM depends mainly on the frequencies at which they will work. In this research, the study of effect of square precipitation on the antenna to obtain the best result. **MTM** are placed over the **supersubstrate** focus with the patch to correct the radiation emitted [19, 20]. After checking the antenna in terms of the first layer, it caused an increase in the outgoing radiation, so the first layer is considered a source was feeding for the second layer, and the second layer caused the radiation to split into two beams and make it more directed [21, 22]. The distance between the layers determines the best possible result, as shown in Table 1. Also, the distance between the layers and the **MTM** is discussed, as illustrated in Table 2, and this inferred distance is the best possible result. In the case of the search for the presence of two layers of the substrate in the manufactured antenna, the distance between the first layer of the ground layer must be $\lambda/3$ [23, 24]. And the distance between the second layer and the first layer, $\lambda/2$ to λ , $\lambda/3$ is the wavelength of the antenna frequency in free space. Therefore, the metamaterials layer of the second layer is the distance $\lambda/4$ [25]. Fig. 4 shows a metamaterial unit cell configuration.

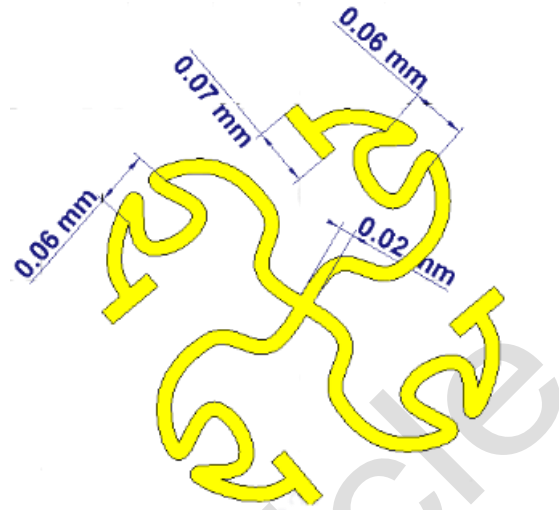


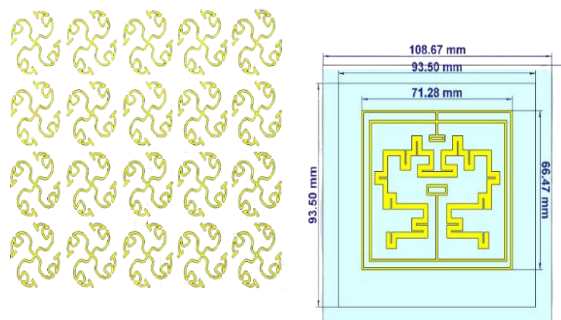
Figure 4: Metamaterial unit cell.

1.4 Superstrate

The aim of designing the **supersubstrate** materials is to enhance and increase the antenna gain by creating a high electric field above the substrate phase. This helps to control the practice of transmitting radiation by making holes inside the Superstrate, which reduces the permittivity. This process is achieved by reducing the front-to-back ratio (FBR), which increases the antenna's efficiency and improves the gain and in turns, achieving the best antenna performance [13, 26].

2 Antenna Configuration

This section describes the design details of the patch antenna with a superstrate placed at an optimum level. The configuration of a three-patches antenna array with the Superstrate is shown in Fig. 5. The lower substrate layer is backed by a ground plane. The overall dimension of the antenna structure is illustrated in Table 1. The space between the lower, upper, and Superstrate is 10.66 mm. Four U-shape patches, each of size $71.28 \text{ mm} \times 66.47 \text{ mm}$, are printed on the upper surface of the upper substrate. The feed is $(-10.5, -2.5)$, with the patch elements fed using a corporate feed with quarter-wave impedance transformers. The lower layer of the Superstrate consists of a patch of square apertures in a ground plane, with the gap between the patch and the metamaterial layer being $d = 29.52 \text{ mm}$.



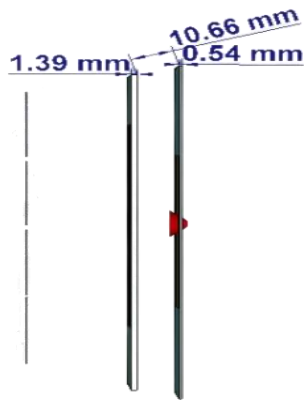


Figure 5: Overall antenna structure.

Table 1: Values of the antenna parameters

Name	Parameter	Value (mm)
Subst 1	A1	108.67
	B1	108.67
Subst 2	A2	93.5
	B2	93.5
Gap between Subst	Hs1	10.6
Thickness of upper substrate	h1	0.54
Thickness of lower substrate	h2	1.39
Patch 1	A	50
	B	50
Patch 2	A	71.28
	B	66.47
Metasurface width	MW	88.24
Metasurface high	MH	88.25
Gap Metasurface and patch 2	Gm	28.25

3 Results and Discussion

To discuss the principal work of the proposed antennas, the designer first understands the effect of antenna structure on the gain and reflection coefficient parameters. So, the antenna in the first part is designed as a rectangle (traditional antenna). Next, the second part is modified using the U-shaped superstructure, followed by the MTM design with a matrix of (5×4) at the last step of the designing process. Finally, the parameters of S are calculated individually for each unit. The three modes are portrayed in Fig. 6. Results obtained in Fig. 7 demonstrated the minimum reflection coefficient achieved at 2.68 GHz.

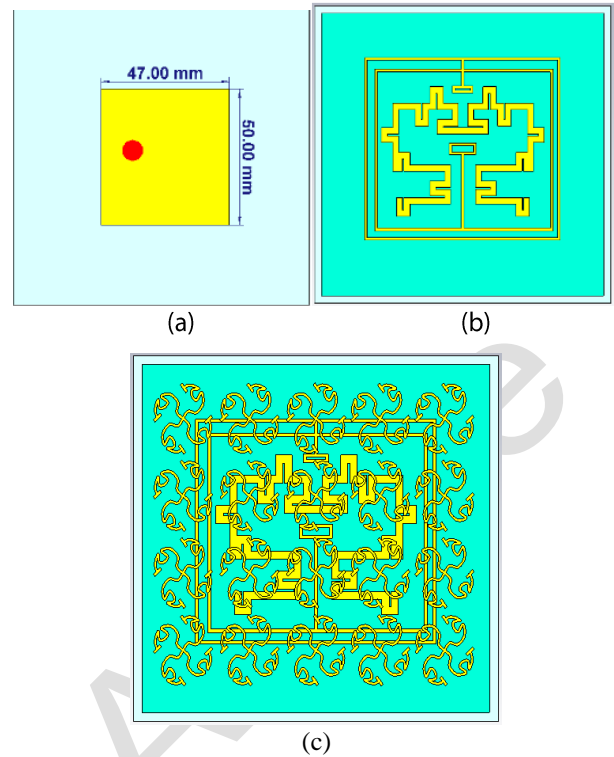


Figure 6: The structure of the antenna (a) patch plane (b) the supersubstrate with U-shape (c) the MTM design.

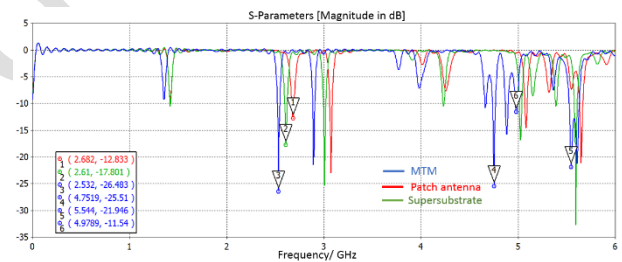


Figure 7: Reflection coefficient results of the proposed antenna at different cases of design.

Moreover, it's noted that the gain is significantly increased to a high value by using the MTM at 5.4 GHz, attained to 8.61 dBi. From the results illustrated in Fig. 8, it is found that the antenna achieves a high gain at the frequencies of 4.7, 4.9, and 5.5 GHz, and this is due to the current distributions between the radiator and the ground plane, which leads to an increase in the gain and bandwidth in the antenna while decreasing the value of the reflection coefficient at certain frequency.

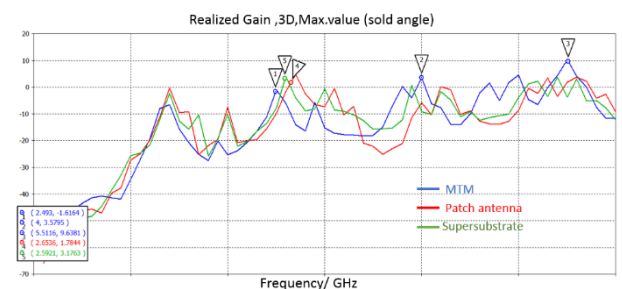


Figure 8: Gain results of the proposed antenna at different cases of design.

To further explain the idea of the split property, Fig. 9 shows the step-by-step evaluation process of the surface current distribution of the antenna. Firstly, the structure proposed of the antenna arranges the split beam property, and the unit cells are rearranged to produce opposite current flow. Then, by observing the current flow for every two cells in one column, the beam is directed differently.

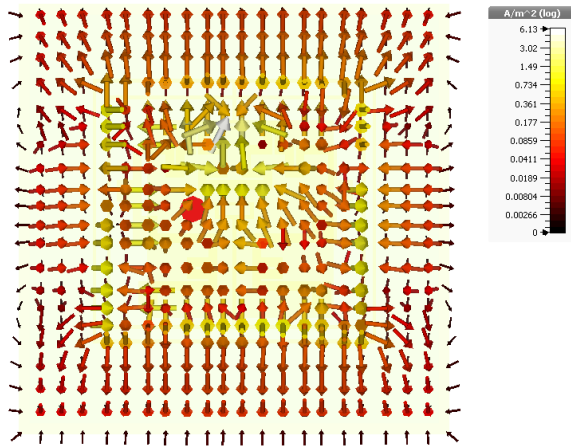


Figure 9: Current distribution of the antenna.

4 Results of Metamaterial Cases

4.1 Even number of MTM arrays

In telecommunication networks, especially antennas, the antenna's dimensions, gain, and reflection coefficient significantly impact the antenna's performance. Hence, this study aims to design and use MTM with an even number or odd arrays for observing the effects on the antenna's efficiency. Based on the results in Fig. 10, matrices significantly improved some frequencies. In this paragraph, the even number is adopted in the MTM matrix, represented as (2×2) , (4×4) , (8×8) , and (10×10) . As a result, as the number of matrices is increasing, the reflection coefficient increases and achieves $(-15.8, -15.8, -10.5, -9.8)$ dB at 2.6 GHz at various matrices sizes.

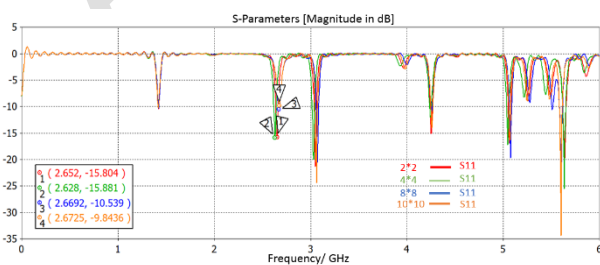


Figure 10: Reflection coefficient results of even MTM.

At a frequency of 2.6 GHz at (4×4) matrix, the result demonstrated a minimum reflection coefficient compared with the rest of the results at other operating frequencies. On the other hand, the gain result at the frequency of 2.6 GHz is 4.33 dBi, as shown in Fig. 11, which also includes the gains result at the rest of the frequencies. For this, results achieved at (4×4) MTM are more acceptable among the other matrices of the even array.

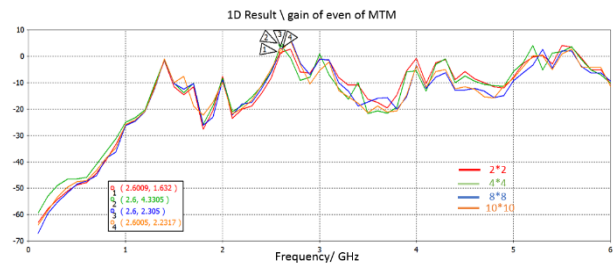


Figure 11: Realized gain results at different MTM even arrays.

4.2 Odd number of MTM arrays

The second part of this section is to make an individual matrix of numbers (3×3) , (5×5) , (7×7) , and (9×9) . The results illustrated that the reflection coefficient parameter at (5×5) is -16.882 dB at 2.6 GHz, as shown in Fig. 12. On the other hand, it's observed that this value is slightly deteriorated at the (9×9) matrix due to the impact of antenna size.

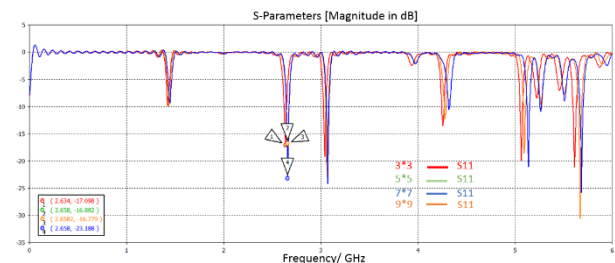


Figure 12: Reflection coefficient results of odd MTM.

In addition, the results show that the (5×5) matrix is more appropriate for achieving a minimum reflection coefficient but with less gain. Thus, at a frequency of 2.6 GHz, the gain attained 1.18 dBi, as shown on Fig. 13. The MTM designing process depends on using the even and odd matrices.

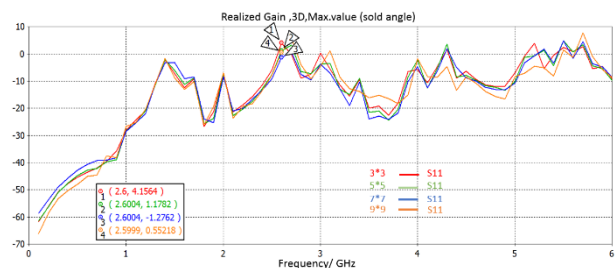


Figure 13: Realized gain results at different MTM odd arrays.

4.3 Hyper MTM array

This section presents the simulation results of the metasurface structure integrated with the antenna. The results obtained using the CST simulator software represent the reflection coefficient and the radiation. Results show that five resonant frequencies were obtained at (2.6, 3, 4.2, 5.2, and 5.6) GHz (see Fig. 14).

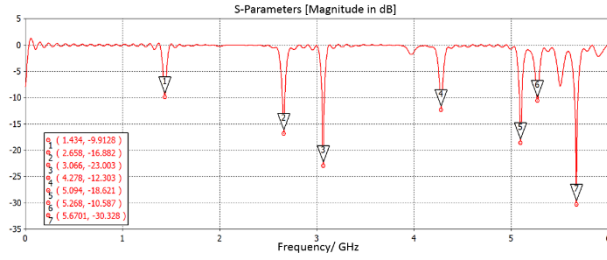


Figure 14: Reflection coefficient results of hyper MTM.

The analysis and simulation in Fig. 15 (a), (b), (c), and (d) indicate that bare **Microstrip patch antenna (MPA)** has a radiation efficiency of 73% at a frequency of 2.6 GHz. The spread beam with the main lobe direction toward is 34 deg. The offender side lobe showed a result of -1.3 dB. At a frequency of 3 GHz, the one beam with the main lobe direction toward is 4 deg, and the offender side lobe showed a result of -17 dB with a radiation efficiency of 99%. Besides that, at a frequency of 4.2 GHz, the one two-beam with the main lobe direction goes toward 27 deg. The offender side lobe showed a -2.3 dB with a radiation efficiency of 32%. Moreover, at the frequency of 5.6 GHz, the one beam with the main route is clearly shown toward 48 deg. Meanwhile, the offender side lobe demonstrated a -3.7 dB with a radiation efficiency of 37%.

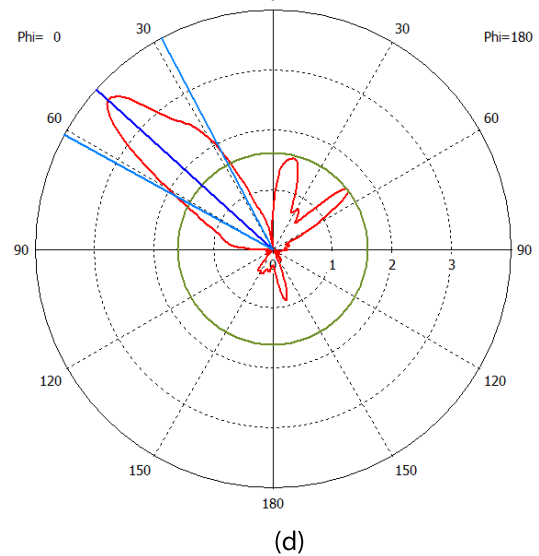
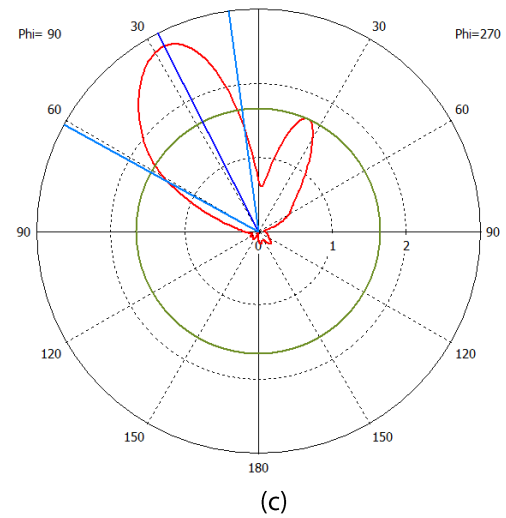
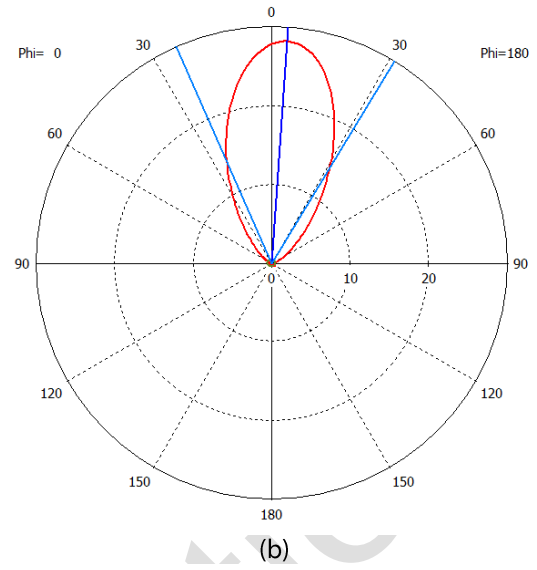
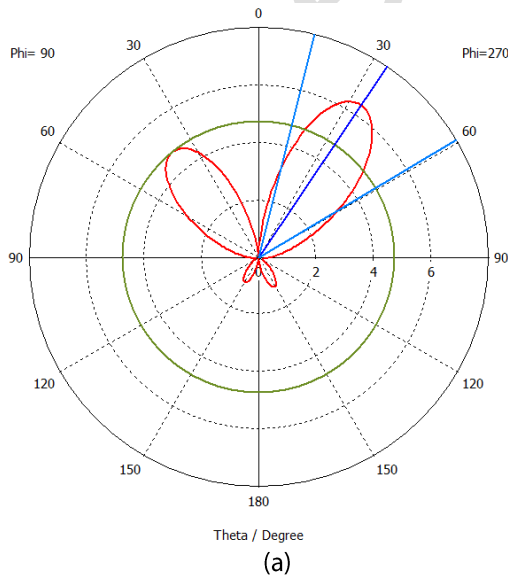
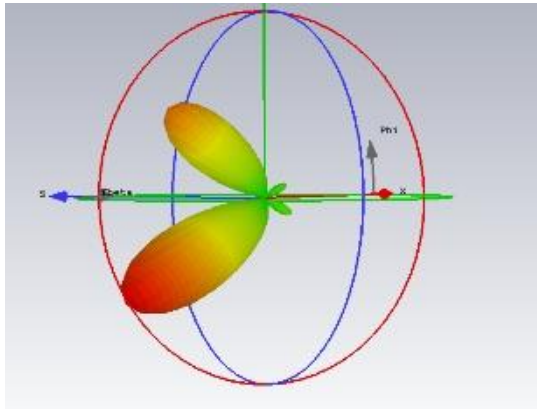
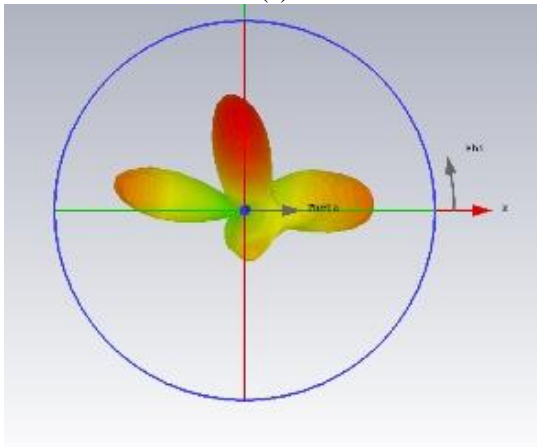


Figure 15: Radiation pattern of the metasurface antenna (a) split beam in 2.6 GHz, (b) one beam in 3 GHz, (c) split beam in 4.2 GHz, (d) split-beam in 5.6 GHz.

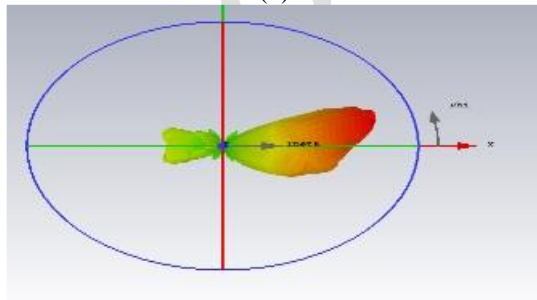
Next, Fig. 16 shows the 3-dimensional results of the antenna, which shows the splitting in the radiation pattern based on the antenna with the MTM structure. Moreover, the antenna proposed in this work is compared with other studies in literature in terms of the operating frequency, antenna dimensions, gain, techniques used, and beam split. This comparison and the overall results of the antenna at different cases of split degrees are summarized in Tables III and IV, respectively.



(a)



(b)



(c)

Figure 16: 3D radiation pattern of the antenna (a): at 2.6 GHz, (b): at 4.2 GHz, (c): at 5.6 GHz.

Table 2: comparison of the proposed antenna with others works in literature

Ref.	Frequency band (GHz)	Size (mm)	Gain (dBi)	Technique	Beam split
[18]	(4.95 - 5.42)	65 × 65 × 4.862	8.62	metasurface	Yes / Two
[26]	3.5	300 × 300	2.3/	MS super-substrate	Yes / Two
[27]	(11.2/12.2)	96 × 13	13	Pin diode / two feed	NO
This work	2.6/4.2 /5.6	108 × 108	8.2/4.49 /6.24	supersubstrate	Yes / Three

Table 3: Summary of the antenna results

fr (GHz)	Reflection coefficient (dB)	Gain (dBi)	Total eff.	Spilt deg.
2.6	-16.8	8.04	76.9%	Two lobs
4.2	-12.3	4.49	84.9%	Three lobs
5.6	-30.6	6.24	83.8%	No lobs

5 Conclusions

This work presented a **MTM** antenna based on **super-substrate** and U-shaped unit cells for improving the antenna's gain and splitting beam. The proposed antenna operates at frequency bands of 2.6 GHz, 4.2 GHz, and 5.6 GHz with a minimum reflection coefficient of -16.8 dB, -12.3 dB, and -30.6 dB, respectively. The proposed antenna is designed and analyzed using the CST MWS. As a result, a gain is improved to 8.04 dBi, 4.49 dBi and 6.24dBi at the broad side of the direction of the antenna at the required impedance bandwidth. In addition, a split beam is significantly observed in the E-plane with a 2.65 dBi gain for each beam.

6 References

- [1] K. Sharma and G. P. Pandey, "A Novel wideband 5G Antenna with Truncated Ground," in *2019 IEEE Indian Conference on Antennas and Propagation (InCAP)*, 2019: IEEE, pp. 1-4.
- [2] M. Abirami, "A review of patch antenna design for 5G," in *2017 IEEE International Conference on Electrical, Instrumentation and Communication Engineering (ICEICE)*, 2017: IEEE, pp. 1-3.
- [3] I. Surjati, S. Alam, Y. K. Ningsih, L. Sari, and J. Tanuwijaya, "Gain Enhancement of Circular Polarization Microstrip Antenna Based on Array 8x2 Element," in *2020 6th International*

- Conference on Wireless and Telematics (ICWT), 2020: IEEE, pp. 1-4.
- [4] W. Hong et al., "Multibeam antenna technologies for 5G wireless communications," *IEEE Transactions on Antennas and Propagation*, vol. 65, no. 12, pp. 6231-6249, 2017.
- [5] B. Q. Elias, M. M. Ismail, B. S. Bashar, A. I. Alanssari, Z. Rhazali, and H. Misran, "Multi-Beam Metasurface Control Based on Frequency Reconfigurable Antenna," *Informacije MIDEM*, vol. 54, no. 2, 2024.
- [6] T. Shaikh, M. Singh, and B. Ghosh, "Gain Enhancement of Patch antenna using Superstrate," in *2021 IEEE Indian Conference on Antennas and Propagation (InCAP)*, 2021: IEEE, pp. 887-889.
- [7] T. Nahar and S. Rawat, "Efficiency enhancement techniques of microwave and millimeter-wave antennas for 5G communication: A survey," *Transactions on Emerging Telecommunications Technologies*, vol. 33, no. 9, p. e4530, 2022.
- [8] U. Kumar, D. K. Upadhyay, and B. L. Shahu, "Improvement of performance parameters of rectangular patch antenna using metamaterial," in *2016 IEEE International Conference on Recent Trends in Electronics, Information & Communication Technology (RTEICT)*, 2016: IEEE, pp. 1011-1015.
- [9] S. S. Bhatia and J. S. Sivia, "Analysis and design of circular fractal antenna array for multiband applications," *International Journal of Information Technology*, pp. 1-11, 2018.
- [10] J. Wang et al., "Metantenna: When metasurface meets antenna again," *IEEE Transactions on Antennas and Propagation*, vol. 68, no. 3, pp. 1332-1347, 2020.
- [11] D.-N. Dang and C. Seo, "High gain antenna miniaturization with parasitic lens," *IEEE Access*, vol. 8, pp. 127181-127189, 2020.
- [12] O. Borazjani, M. Naser-Moghadasi, J. Rashed-Mohassel, and R. Sadeghzadeh, "Design and fabrication of a new high gain multilayer negative refractive index metamaterial antenna for X-band applications," *International Journal of RF and Microwave Computer-Aided Engineering*, vol. 30, no. 9, p. e22284, 2020.
- [13] G. V. R. Xavier, A. J. R. Serres, E. G. da Costa, A. C. de Oliveira, L. A. M. M. Nobrega, and V. C. de Souza, "Design and application of a metamaterial superstrate on a bio-inspired antenna for partial discharge detection through dielectric windows," *Sensors*, vol. 19, no. 19, p. 4255, 2019.
- [14] A. Labiad, K. Bouras, and M. Bouzouad, "Metamaterials Reconfigurable Multiband Antenna," *Advanced Science, Engineering and Medicine*, vol. 11, no. 11, pp. 1097-1099, 2019.
- [15] S. Glinsek, V. Furlan, T. Pecnik, M. Vidmar, B. Kmet, and B. Malic, "Elliptically polarized frequency agile antenna on ferroelectric substrate," *Informacije MIDEM*, vol. 48, no. 4, pp. 229-233, 2018.
- [16] P. D. Sinha, B. Ghosh, and B. Deepa, "Gain Enhancement of Patch Antenna Array Using a Metamaterial Superstrate," in *2021 IEEE International Symposium on Antennas and Propagation and USNC-URSI Radio Science Meeting (APS/URSI)*, 2021: IEEE, pp. 251-252.
- [17] P. D. Purnamasari and F. Y. Zulkifli, "Gain Enhancement of Microstrip Antenna Using Genetic Algorithm: A Review," in *2021 International Conference on Radar, Antenna, Microwave, Electronics, and Telecommunications (ICRAMET)*, 2021: IEEE, pp. 166-171.
- [18] Z. Zhao and W. Zhang, "Multi-beam antenna based on annular slot and uneven metasurface," *International Journal of RF and Microwave Computer-Aided Engineering*, vol. 31, no. 11, p. e22814, 2021.
- [19] S. Palekar and N. Rao, "Miniaturization and Gain Enhancement of Rectangular Patch Antenna Using CSRR," in *Optical and Wireless Technologies: Proceedings of OWT 2020*, 2022: Springer, pp. 269-279.
- [20] S. K. Patel, S. P. Lavadiya, J. Parmar, K. Ahmed, S. A. Taya, and S. Das, "Low-cost, multiband, high gain and reconfigurable microstrip radiating structure using PIN diode for 5G/WiMAX/WLAN applications," *Physica B: Condensed Matter*, vol. 639, p. 413972, 2022.
- [21] M. Atanasijević-Kunc, V. Kunc, and M. Štiglic, "AUTOMATIC TUNING OF ELECTRICAL SMALL ANTENNAS," *Informacije MIDEM*, vol. 40, no. 3, pp. 174-177, 2010.
- [22] T. Pavani, A. Hemanth, I. S. Narayana, and Y. R. Rao, "Patch or Microstrip Antenna using Metamaterials: A Review," in *2021 Third International Conference on Intelligent Communication Technologies and Virtual Mobile Networks (ICICV)*, 2021: IEEE, pp. 54-57.
- [23] R. Ge, "A Study of Conformal Metasurfaces on Passive Beam Steering for Arrays," North Dakota State University, 2022.
- [24] B. Q. Elias, M. Alsajri, P. J. Soh, and A. A. Al-hadi, "Design of Flexible Planar Antennas Using Substrate Gap Structure for Surface Wave Reduction," in *2019 22nd International Conference on Control Systems and Computer Science (CSCS)*, 2019: IEEE, pp. 453-458.
- [25] T. Z. Fadhil, N. A. Murad, M. K. A. Rahim, M. Hamid, and L. O. Nur, "A beam-split metasurface antenna for 5G applications," *IEEE Access*, vol. 10, pp. 1162-1174, 2021.
- [26] Z. Mousavirazi, V. Rafiei, and T. A. Denidni, "Beam-switching antenna array with dual-circular-polarized operation for WiMAX applications," *AEU-International Journal of*

- Electronics and Communications*, vol. 137, p. 153796, 2021.
- [27] B. S. Bashar *et al.*, "Antenna beam forming technology based enhanced metamaterial superstrates," in *2022 IEEE 3rd KhPI Week on Advanced Technology (KhPIWeek)*, 2022: IEEE, pp. 1-5.



Copyright © 20xx by the Authors.
This is an open access article distributed under the Creative Commons Attribution (CC BY) License (<https://creativecommons.org/licenses/by/4.0/>), which permits unrestricted use, distribution, and reproduction in any medium, provided the original work is properly cited.

Arrived: 08.10.2024

Accepted: 05.03.2025

Accepted Article